Understanding Local-Field Correction Factors in the Framework of the Onsager–Böttcher Model

Antoine Aubret[†*] Michel Orrit[‡] Florian Kulzer[§*]

December 7, 2018

1 Abstract

The determination of the appropriate local-field factor for quantifying the response of a molecule to an external electric field is of major importance in optical spectroscopy. Although numerous studies have dealt with the evolution of the optical properties of emitters as a function of their environment, the choice of the model used to quantify local fields is still ambiguous, and sometimes even arbitrary. In this paper, we review the Onsager–Böttcher model, which introduces the polarizability of the probe molecule as the determinant parameter for the local field factor, and we establish a simple conceptual framework encompassing all commonly used models. Finally, a discussion of published experimental research illustrates the potential of the measurement of local electric fields in dense dielectric media, as well as the subtleties involved in their interpretation.

2 Introduction

When molecules and other small structures are subjected to an externally applied electric field, they experience local fields that differ from the measurable macroscopic ones in non-trivial manners. This effect can be taken into account quantitatively by so-called local-field corrections, which are required to relate the optical response of the molecule to its properties as observed in vacuum or a different medium. A particularly important domain of applications of local-field corrections is optical spectroscopy [1, 2], given that the optical properties of emitters strongly depend on their dielectric environment. This exquisite sensitivity is, at the same time, a promising opportunity and a significant challenge for applications like designing photonic materials [2–4] or using emitters as nanoprobes [5–9]. In all such endeavors, a precise understanding of the local field acting on the optically active entities is of primary importance.

[†]Dr. A. Aubret, University of California San Diego (UCSD), Physics Department, 9500 Gilman Dr., La Jolla, CA 92093 – 0319, USA

[‡]Prof. Dr. M. Orrit, Molecular Nano-Optics and Spins (MoNOS), Huygens Laboratory, Leiden University, P.O. Box 9504, 2300 RA Leiden, The Netherlands

[§]Prof. Dr. F. Kulzer, Institut Lumière Matière, CNRS UMR5306, Université Lyon 1, Université de Lyon, 69622 Villeurbanne CEDEX, France

*corresponding authors: aaubret@ucsd.edu, florian.kulzer@univ-lyon1.fr

In this paper, we develop a simplified electrostatic description based on Böttcher's treatment of a point dipole in an empty spherical cavity in a linear and isotropic dielectric medium, which establishes a unifying conceptual framework for understanding the relationship between the commonly used local-field models. We furthermore discuss extensions of the simple model, covering special cases such as non-spherical molecules and inhomogeneous or absorbing media, and we briefly review complementary approaches based on microscopic models and quantum-mechanical treatments in the light of their applications in optical experiments. We then connect the theoretical descriptions to experimental studies involving different types of nano-objects, which serves both as an illustration of the discussed models and as a demonstration of the potential of single-emitter spectroscopy in dielectric media.

3 The Onsager–Böttcher treatment of a dipole in a cavity

The evaluation of local-field corrections is a complex and long-standing problem, which in general requires a careful consideration of the vectorial nature of the field and of its inhomogeneous distribution at molecular scales [10]. A simplified macroscopic model commonly used to calculate local-field corrections considers the molecule of interest as a static point-dipole situated at the center of a spherical cavity that is immersed in a continuous, homogeneous surrounding medium. This concept was first introduced by Bell in 1931 to describe molecules in liquid media [11]. Such an electrostatic model can also be applied to optical fields, provided the cavity diameter is much smaller than the wavelength of light (which is usually the case for molecules and nanoparticles), meaning that retardation effects can be neglected.

Upon application of a macroscopic field along the z-axis (see Fig. 1), polarization charges are induced on the surface of the spherical cavity. These charges create an additional field, which contributes to the polarization of the dipole. In return, the point dipole itself polarizes the solvent outside the cavity, thereby further modifying the polarization charges. This coupled problem cannot easily be solved by linear superposition arguments and must be addressed in a self-consistent manner.

We thus consider a point dipole at the center of a spherical cavity with radius R, surrounded by a linear and isotropic medium with relative dielectric constant ϵ. Given that the dielectric is isotropic, all vectors will be directed along the applied field and we write their algebraic values only. The Onsager-Böttcher treatment holds for static dipoles and polarizabilities. We focus here on its implication in optical and spectroscopic experiments, and therefore consider only the polarizability, which is the relevant parameter in experiments. (The case of a permanent static dipole component of the host molecule will briefly be addressed later.) The dipole moment μ of the central point dipole is related to its polarizability χ by

$$\mu = \chi E_{\mathrm{loc}} \quad , \tag{1}$$

where E_{loc} is the local field experienced by the dipole, resulting from all external charges. This consideration includes the far-away charges polarizing the medium (symbolized as capacitor plates in Fig. 1) and the polarization charges at the

boundary of the cavity, which have to be adjusted such that a self-consistent description of all polarization effects is achieved. Furthermore, the polarizability of the solute may change due to electrostatic and specific interactions with the medium molecules, which affect electronic transition energies and transition dipole matrix elements. A refined local-field correction should therefore also take theses changes of polarizability into account in a self-consistent way. For the sake of pedagogical clarity, however, we will neglect these higher-order terms in the following discussion, which amounts to assuming the polarizabilities of the solute and solvent molecules to be constant and equal to the corresponding vacuum values.

Finding the general solution for the electrostatic potential V in the geometry of Fig. 1 is a standard problem of electrostatics, determined by the Laplace equation for the electric potential, $\Delta V = 0$. Given the rotational symmetry of the cavity model, the general solution can be expressed in spherical polar coordinates (with the applied field and dipole parallel to the z-axis) as a sum of terms composed of a radial function $f(r)$ multiplied with a Legendre polynomial in $\cos\theta$, where θ is the polar angle [12]. For the specific problem considered here, the derivation of the potential can be simplified by noting that we are only interested in solutions whose angular dependence corresponds to the potential of the combination of a uniform field with a dipole field, both of which vary as $\cos\theta$. The radial Poisson equation thus reduces to

$$\frac{d}{dr}\left(r^2\frac{df(r)}{dr}\right) - 2f(r) = 0 \quad , \tag{2}$$

which admits two linearly independent solutions, $f(r) = r$ and $f(r) = 1/r^2$, corresponding to a uniform field and a dipole field, respectively, when combined with the $\cos\theta$ term. The most general potentials inside (V_{in}) and outside (V_{out}) the spherical cavity are written as linear combinations of these two solutions:

$$V_{\mathrm{in}} = \left[a + b\left(\frac{R}{r}\right)^3\right] r\cos\theta \tag{3}$$

$$V_{\mathrm{out}} = \left[A + B\left(\frac{R}{r}\right)^3\right] r\cos\theta \tag{4}$$

For the sake of generality, we assume the inside of the sphere to be a dielectric with relative permittivity ϵ_1 while the outside medium is a dielectric with permittivity ϵ_2. There are three consistency and boundary conditions that determine the unknown coefficients in Eqs. (3) and (4): First, the continuity conditions at the surface of the sphere ($r = R$) for the potential and for the normal (radial) component of the electric displacement vector, $D_{\mathrm{in/out}} = -\epsilon_0\epsilon_{1/2}\nabla V_{\mathrm{in/out}}$, which impose

$$\begin{aligned} a + b &= A + B \\ \epsilon_1(a - 2b) &= \epsilon_2(A - 2B) \quad . \end{aligned} \tag{5}$$

Second, the boundary conditions at infinity and at the origin,

$$\begin{aligned} A &= -E_{\mathrm{m}} \\ b &= \frac{\mu}{4\pi\epsilon_0\epsilon_1 R^3} \quad , \end{aligned} \tag{6}$$

where E_m is the incident field applied by the far-away electrodes and therefore independent of the microscopic details of the sphere; μ is the dipole moment at the center of the cavity, whose potential is $\mu\cos\theta/(4\pi\epsilon_0\epsilon_1 r^2)$. Finally, there is the constitutive equation of the dipole relating its moment to the local electric field that it experiences, which here is the uniform field created in the cavity (the dipole does not act on itself):

$$\mu = \chi E_\mathrm{loc} = -\chi a \quad . \tag{7}$$

Eliminating B, we obtain the local field correction factor, i. e., the ratio of the local field to the applied far-away macroscopic field, as:

$$L = \frac{E_\mathrm{loc}}{E_\mathrm{m}} = \frac{3\epsilon_2}{\epsilon_1 + 2\epsilon_2 - \frac{2}{3}\frac{\epsilon_2-\epsilon_1}{\epsilon_1}\frac{\chi}{\epsilon_0 V_\mathrm{I}}} \tag{8}$$

where $V_\mathrm{I} = \frac{4}{3}\pi R^3$ is the volume of the cavity occupied by the molecule; note that the local field factor depends on the ratio of the dipole polarizability χ and the inclusion volume V_I, i. e., the polarizability density. In the following, we consider a few special cases, which will elucidate the physical interpretation of this relation and illustrate the relationship between the various local-field correction factors used in the literature.

3.1 The empty cavity

The empty-cavity (EC) field correction factor L_ec arises in the quantum optical treatment of dielectric media presented by Glauber and Lewenstein [13]. We find the same field correction factor when we apply Eq. (8) to an empty spherical cavity in medium ϵ_2 by setting $\epsilon_1 = 1$ and $\chi = 0$:

$$L_\mathrm{ec} = \frac{3\epsilon_2}{2\epsilon_2 + 1} \tag{9}$$

This model is in general recovered when the polarizability density $\chi/(\epsilon_0 V_\mathrm{I})$ tends to zero.

3.2 A dielectric sphere in vacuum

We can apply the model to the response of a dielectric sphere in vacuum that is subjected to a macroscopic electric field E_m. The sphere will behave as an equivalent dipole with a moment M, which, in the formalism of Eq. (4), is given by $M = 4\pi\epsilon_0 R^3 B$. Putting $\epsilon_2 = 1$ (vacuum) and $\chi = 0$ (no additional point-dipole is present in the sphere, which also implies $b = 0$), we can solve Eqs. (5) and (6) for B to obtain:

$$M = 4\pi\epsilon_0 R^3 \frac{\epsilon_1 - 1}{\epsilon_1 + 2} E_\mathrm{m} \tag{10}$$

This well-known relation describes the optical response of an isotropic dielectric sphere to a uniform field and provides the lowest-order electrostatic approximation of the equivalent polarizability α_e in Mie theory [14]:

$$\alpha_\mathrm{e} = 4\pi\epsilon_0 R^3 \frac{\epsilon_1 - 1}{\epsilon_1 + 2} \tag{11}$$

3.3 The Lorentz-Lorenz relation

The Lorentz-Lorenz relation is the standard textbook illustration of local-field effects. The usual derivation of this formula starts by decomposing the dielectric medium into its constituent dipoles, typically arranged on a cubic lattice, and introducing an imaginary cavity to find the local field at the lattice points. The local field then turns out to be determined by the surface charges at the boundary of the cavity, while, somewhat counter-intuitively, the nearest-neighbor dipoles in the cavity contribute nothing to the field due to accidental cancellations arising from the cubic lattice symmetry; a full discussion of these conceptual issues can be found in Ref. [15]. We can treat the same problem in a straightforward manner by considering a dielectric medium with an embedded sphere of the *same* dielectric material, which simply means replacing the polarizable dipole at the center of the cavity in Fig. 1 by the dielectric sphere of Section 3.2, this time with the identical dielectric constant ϵ_2 and the associated polarizability $\alpha'_{\rm e} = 4\pi\epsilon_0 R^3 \frac{\epsilon_2-1}{\epsilon_2+2}$ analogous to Eq. (11). We thus find the Lorentz local-field correction (also known as the virtual cavity model) [16] $L_{\rm L}$:

$$L_{\rm L} = \frac{E_{\rm loc}}{E_{\rm m}} = \frac{3\epsilon_2}{1+2\epsilon_2 - 2\frac{\epsilon_2-1}{4\pi\epsilon_0 R^3}\alpha'_{\rm e}} = \frac{\epsilon_2+2}{3} \tag{12}$$

This well-known expression of the local field is equivalent to the Clausius-Mossotti relation between polarizability and dielectric permittivity: $(\alpha/3\epsilon_0\Omega) = (\epsilon_2-1)/(\epsilon_2+2)$, where Ω is the volume occupied by each of the constituent molecules.

It is remarkable that we obtain the Lorentz-Lorenz relation without having to introduce any point dipoles – we just replaced the field of a sphere by that of a point dipole in the region outside the sphere, which is an exact solution of Maxwell's equations. No decomposition of the medium into dipoles and no accidental cancellation of dipole fields are required to obtain this relation. The Lorentz-Lorenz relation above is thus simply a *consistency condition* for representing a homogeneous medium by an isotropic dielectric: If a medium is homogeneous and isotropic, then the Lorentz-Lorenz condition must be obeyed.

3.4 The Onsager–Böttcher model

As pointed out by Böttcher [17] based on the initial work of Onsager in 1936 [18], the local-field correction factor depends on the polarizability χ of the molecule placed in the cavity. We therefore now consider a polarizable point dipole at the center of an empty cavity in dielectric medium ϵ_2. It is instructive to rewrite the polarizability of the dipole as a variation δ of the equivalent polarizability $\alpha = \alpha'_{\rm e}$ of the sphere that was removed when forming the cavity: $\chi = \alpha + \delta$. For positive δ, the dipole in the center of the cavity is more polarizable than the removed dielectric, which will generally be the case in spectroscopy of solvated molecules at optical frequencies.

For a homogeneous distribution of the polarizability in the spherical cavity, one can choose the volume to be that of the host, i.e., $V_{\rm I} = \Omega$, and the polarizability will adjust itself accordingly. This consideration can also be extended to the case of a point-dipole at the center of a spherical cavity, due to the equivalence of the reaction fields for, respectively, a sphere filled with dielectric material and a single point dipole inside an empty cavity [17].

Using the Clausius-Mossotti relation as given in Section 3.3, we find the local field correction factor L_{B}:

$$L_{\mathrm{B}} = \frac{L_{\mathrm{L}}}{1 - 2\frac{(\epsilon_2 - 1)^2}{9\epsilon_2}\frac{\delta}{\alpha}} \tag{13}$$

We thus see that the local field correction factor increases when the solute is more polarizable than the solvent, and we note that Eq. (13) includes the empty and virtual cavity models for $\delta = -\alpha$ and $\delta = 0$, respectively; a graphical comparison is shown in Fig. 2.

3.5 Choice of model

We now discuss some guidelines for the choice of model depending on the nature of the dipole inside the cavity. For pure systems constituted of only one kind of atom, or when the polarizability of the guest is the same as that of the host, the Lorentz model (virtual cavity) should apply. On the other hand, when the polarizability of the guest dipole is sufficiently low compared to that of the host, the reaction field caused by the induced dipole acting on the cavity can be neglected and the empty cavity model applies. The EC model thus represents a lower boundary for the local field factor. In the general case of a guest with arbitrary polarizability, the appropriate local-field factor is given by the Onsager–Böttcher model, Eq. (13), which, as has been pointed out above, contains the EC and VC models as special cases. However, Eq. (13) clearly becomes invalid when δ is too large, as the denominator will vanish. In that case, the solute-solvent system can become unstable and acquire polarization spontaneously, upon a ferro-electric phase transition, for example; of course, the linear approximation ceases to apply in that case [19]. The model described above thus remains valid only for a polarizability difference $\delta < 9\epsilon_2\,\alpha/[2(\epsilon_2 - 1)^2]$.

3.6 Implications for optical experiments

As can be appreciated directly from Fig. 2, the various local-field factors imply significant differences of an emitter's sensitivity to a change in the local refractive index, meaning that the validity of any given model should be easily verifiable if the same species can be studied in a series of media with sufficiently distinct refractive indices. Therefore, experiments dealing with local-field effects most commonly rely on the analysis of absorption spectra or the dynamics of spontaneous emission (luminescence lifetime) as a function of the surrounding dielectric medium. Briefly, in spontaneous emission, the emitter couples to the local field when immersed in a homogeneous medium of dielectric constant ϵ_2. The general expression for the radiative decay rate of an emitter is obtained from Fermi's Golden Rule as $\Gamma_{\mathrm{r}} = \sqrt{\epsilon_2}\,\Gamma_{\mathrm{r},0}$ [20], where $\Gamma_{\mathrm{r},0}$ is the radiative decay rate in vacuum. Taking into account local field corrections, the radiative decay rate is given by $\Gamma_{\mathrm{r}} = \sqrt{\epsilon_2}\,L^2\,\Gamma_{\mathrm{r},0}$, where L is the applicable local-field factor [1]. Exploring the relative variation $\Gamma_{\mathrm{r}}/\Gamma_{\mathrm{r},0}$ thus yields information on the local field experienced by the emitter.

There is, however, a complication as soon as the emission quantum yield differs significantly from unity. The observed overall fluorescence decay rate is then given by the sum of the radiative and the non-radiative decay rates,

$\Gamma = \Gamma_\mathrm{r} + \Gamma_\mathrm{nr}$, and it is generally assumed that only Γ_r depends on the local field according to one of the models outlined above. Consequently, the extent of the non-radiative contribution has to be known for a quantitative analysis, or the quantum yield has to be introduced as an additional adjustable parameter. Furthermore, it may not always be straightforward to rule out changes of Γ_nr in different matrices, for example due to a modified geometry of a guest molecule or due to its potential coupling to dissipative degrees of freedom of the matrix.

In optical spectroscopy, the amplitude of optical fields are usually small enough so that the linear response approximation applies, which justifies interpreting experimental results in the framework of the Onsager-Böttcher model. However, some optical experiments involve a strong coupling of light with the medium, giving rise to nonlinear optical effects such as second-harmonic generation, the Kerr effect or four-wave mixing. Quadratic and higher-order terms of the local electric field become significant in all these cases, and it is therefore crucial to apply field-correction factors that take into account higher-order polarizabilities (hyperpolarizabilities) in a self-consistent manner [21–23].

3.7 Extended models

We will now discuss models going beyond the framework of a spherical inclusion cavity, which explicitly take into account deviations from a spherical geometry or attempt to describe the external field effects at the microscopic level of individual atomic or molecular dipoles.

3.7.1 Anisotropy of solute and solvent molecules

For most polyatomic molecules, spherical symmetry is not a good approximation; if such a guest molecule cannot rotate freely due to solute-solvent interactions then an elongated cavity must be used to model local-field effects. A generalization of Eq. (13) for an ellipsoidal cavity can be found in Ref. [17]: Dimensionless scale factors a, b, and c are defined such that the principal axes of the ellipsoid are given by aR, bR and cR, respectively, and a form factor L_μ ($\mu = a, b, c$) is introduced to quantify the contribution to the screening of the electric field along each axis. One can then discuss two distinct cases, either a homogeneous polarizability filling the whole cavity or a point dipole at the center of the cavity.

In the first case, with the interior of the cavity having a polarizability χ_c along the c-axis, the local-field correction factor is found to be [17, 24]

$$L_\mathrm{B} = \frac{\epsilon_2}{\epsilon_2 + (1-\epsilon_2)L_c - 3L_c(1-L_c)\frac{(\epsilon_2-1)\chi_c}{4\pi\epsilon_0 abcR^3}} \quad , \tag{14}$$

where the form factor L_c is given by

$$L_c = \frac{abc}{2}\int_0^\infty \frac{ds}{(s+c^2)\sqrt{(s+a^2)(s+b^2)(s+c^2)}} \quad . \tag{15}$$

We note that in the case of a spherical cavity, $a, b, c = 1$, the three form factors are identical, $L_\mu = 1/3$, and Eq. (13) is recovered; setting $\chi_c = 0$, on the other hand, yields the local-field factor for an empty ellipsoidal cavity. As mentioned earlier, the reaction field of a point dipole at the center of a sphere is identical

to the field created by a homogeneous sphere with same polarizability. This equivalence is lost when dealing with ellipsoidal cavities as the resulting reaction field is non-homogeneous and requires more intricate calculations. Eq. (14) constitutes the first-order term in the development of the reaction field due to a dipole at the center. It should furthermore be noted that, due to the reduced symmetry of an ellipsoidal cavity, the induced dipole moment will not necessarily be parallel to the external field. The relation (14) thus only holds for an emitter filling up the entire cavity, such as a molecule with its transition dipole moment along the long axis, or for an emitter with same polarizability as the cavity. The absorption properties of quantum-confined elongated structures in which the absorption dipole is delocalized inside the core can also be understood in this framework. On the contrary, Eq. (14) ceases to be applicable if there is empty space in the cavity, as is the case for rare-earth-doped nanoparticles in an elongated cavity, distorted micelles or droplets around emitters, or holes in solids with single point dipoles, for instance. In all these situations, Eq. (14) is valid for point dipoles in the low-polarization limit only.

Guest molecules are often assumed to be incompressible so that their van der Waals radii can be used directly in Eqs. (13) and (14). However, non-negligible compression or extension effects do occur in solids and dense liquids. For instance, a molecule with a fixed polarizability density will experience a local-field factor that is reduced by a factor of two when an elongated cavity of axes $a, b = 1,\ c = 3$ is considered instead of a spherical one $(a, b, c = 1)$ [24]. In case of ions embedded in solid matrices, distortion effects can even compete with the influence of the change in refractive index represented by the host medium [25].

As the medium generally changes the electronic distribution of the probe molecule in condensed phases, it may be preferable to reason in terms of effective molecular properties (dipole moments, polarizabilities, etc.) in a given medium [21], different from their vacuum counterparts, which serve as the staring point for incorporating the effects of external fields. Such effective molecular properties must also include a static dipole contribution when applicable. One must thus take care to disentangle the local-field effects from all other phenomena that influence the optical properties of the guest before interpreting the results with a standard spherical-cavity model, even when comparing media of identical refractive indices.

Finally, in the most general case when the shape of the cavity is neither spherical nor ellipsoidal, the field is not uniform and higher-order multipoles have to be considered to achieve an adequate description [1]. In the derivation of Eq. (13), we furthermore neglected any local anisotropy or deformability of the medium. In the more general case of anisotropic permittivity and polarizability, local-field factors can be derived from a tensorial treatment [26]. Similar considerations apply to the case of a polarizable solute with a permanent dipole moment, which can be accommodated by replacing the constitutive relation of Eq. (7) with $\mu = \mu_0 \hat{\mathbf{u}} + \chi \mathbf{E}_{\mathrm{loc}}$, where $\hat{\mathbf{u}}$ is a unit vector representing the orientation of the permanent dipole μ_0. In this situation, a reaction field is present even in the absence of any external field; its effect can be important, especially in polar solvents, where the solvent molecules fully orient and the static dielectric constant has to be considered.

3.7.2 Microscopic models

We will now briefly review models that go beyond the continuum approach adopted so far, in that they explicitly take into account the microscopic entities (atoms, ions, molecules) that make up the host matrix instead of treating it as a homogeneous medium characterized by a macroscopic dielectric constant ϵ. The constituents of the host can be modeled as classical electric dipoles or treated as quantum-mechanical systems.

In the framework of classical electrodynamics, one typically calculates the back-scattered field at the position of the emitter to determine the induced modification of the radiative relaxation rate Γ_r [27], which can then be compared to measured fluorescence decay curves. However, this approach usually overlooks the local field induced by the dielectric medium in which the emitter is embedded and considers mainly the modifications of the local density of photon states due to reflections at boundaries between regions of different ϵ. An Onsager-based approach has been proposed by Cao et al. [28], and further expanded by Tomaš in 2003 [29]. This scheme places an oscillating dipole in the center of an empty spherical cavity and predicts a modification of the spontaneous emission rate compatible with the empty-cavity local-field correction factor. The agreement found here is a consequence of an analogy between the transition dipole moment of an emitter and a polar, non-polarizable dipole moment that is subjected to its own reaction field. In the latter case one can consider the external dipole moment μ^*, which generates the dipole field outside of the cavity, and one finds that, without an externally applied field, the modification of μ^* corresponds to the empty-cavity factor of (9), i. e., $\mu^*/\mu = L_\mathrm{ec}$ [18]. Transferring this result to the classical expression for the radiative decay rate in a homogeneous medium evidently recovers the empty-cavity factor for spontaneous emission.

The polarizability of a fluorescent molecule in transition between the excited and ground states is, strictly speaking, undefined at optical frequencies, and its effects on the reaction field are therefore often neglected. One thus represents an emitter as a rigid permanent dipole, akin to a polar molecule, interacting with its own scattered field. Cao et al. furthermore showed that quantum-analytical calculations neglecting the reaction field predict the same spontaneous emission rate as the classical Onsager-based approach [28]. This manner of treating the emission process agrees with the simple picture of vacuum fluctuations playing the role of the externally applied field on an empty cavity in a homogeneous medium. The comparison of the two descriptions rests on a correspondence relation between the classical dipole moment and the quantum-mechanical transition dipole moment; it turns out that the well-known correspondence relationship applicable to spontaneous emission in vacuum ensures the compatibility of the Onsager–Böttcher model with the approach of Cao et al. However, the physical meaning of this reaction-field-free quantum-mechanical description remains somewhat unclear. In fact, the excited state is more polarizable than the ground state for most molecules, while it is not necessarily permanently polarized. The two scenarios are thus able to describe spontaneous emission for non-polarizable emitters, but further theoretical efforts are needed to extend it to highly polarizable species.

We note that there is an alternative to interpreting the modification of the decay rate in terms of a modification of the electromagnetic density of states (embodied by the spherical cavity) in an inhomogeneous medium: One can in-

stead consider a modified effective dipole comprised of the solute and a few layers of guest molecules, which is then immersed in normal medium [24]. Depending on the nature and geometry of the system, it may be preferable to use one or the other picture.

In 1998, De Vries and Lagendijk [30] proposed a fully microscopic model based on resonant classical light scattering by impurity atoms in dielectric cubic lattices, applied to the dynamics of spontaneous emission; this problem was treated with a combined transfer matrix and Green's function approach. Two years later, Schuurmans and Lagendijk recovered the earlier results from a simpler macroscopic approach [31], based on the Onsager–Böttcher model described previously. This latter approach considers the total polarizability of the (empty) cavity that is generated inside the dielectric due to the impurity atom and then calculates the dipole potential outside the cavity, which is found to correspond to the polarizability:

$$\alpha_{\mathrm{cav}} = \chi L_{\mathrm{ec}} L + (1-\epsilon) L_{\mathrm{ec}} V_{\mathrm{I}} \quad , \tag{16}$$

where L and L_{ec} are given by Eqs. (8) and (9), respectively. The first term of Eq. (16) represents the dipolar field induced by the impurity inside the cavity, and the second one quantifies the response of the cavity to the applied field. The Schuurmans-Lagendijk approach then uses the optical theorem, which relates the extinction cross section of the emitter to the re-distributed energy. By expressing the dynamic polarizability of the cavity formed by the atom, one can extract the resonance linewidth, or damping rate, taken to be equivalent to the radiative decay rate Γ_{r} of the emitter. At this point, interstitial and substitutional inclusion are distinguished by Schuurmans and Lagendijk. For interstitial impurities, the many-particle correlations between the atoms in the matrix are treated as unchanged by the authors, meaning that the impurity experiences an electric field according to the virtual cavity (Lorentz) local-field factor, Eq. (12). A substitutional impurity, on the other hand, which perturbs the matrix by substituting a lattice site, is considered to be subject to the empty cavity local-field factor of Eq. (9). The conclusion for fluids is that the substitutional case should mainly occur, since the emitters often expel the solvent, while for solids both cases (interstitial or substitutional) can happen. For gases, finally, the distinction is irrelevant since the development at the first order of the models is the same.

Crenshaw and Bowden [32] proposed a microscopic model that considers the interactions between an embedded emitter and the atoms of the dielectric medium (treated as two-level systems) at the microscopic level to find an approximated (first-order) solution for the equation of motion of the excited state of the guest. In this framework one finds a dependency of the local-field factor on the refractive index of the host that is even weaker than the one of the empty-cavity model shown in Fig. 2. Furthermore, the Crenshaw–Bowden approach predicts a different slope at $n = 1$ for the curve of Γ_{r} as a function of n. More critically, it results in anisotropic refractive indices for perfectly isotropic media, as pointed out by Berman and Milonni [33]. The latter authors present a refined model that takes into account magnetic sublevels of the atoms in the environment, and for which both the virtual-cavity and the empty-cavity description are consistent for dilute gases ($n \to 1$). These calculations were extended to second order of a simplified Hamiltonian by Fu and Berman in 2005 [34], who

find that only the virtual-cavity model is consistent with their refined model. A theoretical comparison published by Crenshaw in 2008 [35] likewise concluded that microscopic theory of quantum electrodynamics is in agreement with the classical approach to local-field correction, *i.e.*, the virtual-cavity model. While these combined theoretical efforts have undoubtedly advanced the fundamental understanding of local field correction factors, a significant limitation for their application to experimental data is that they are applicable to highly dilute gases only. For a general overview of quantum-chemical solvation models, see the review by Tomasi et al. [36].

3.7.3 The effect of inhomogeneous and absorbing media

The macroscopic models discussed so far have neglected local inhomogeneities around the dipole, assuming an homogeneous and isotropic surrounding medium. Deviations to all the models discussed above are expected to arise due to a grainy nature of the solvent, or more generally due to local inhomogeneities around the emitter of interest. Thermal fluctuations do occur, in solvents or solid matrices. Defects in crystals are unavoidable and can furthermore be induced by the very presence of the impurity atom or molecule itself, and likewise must be accounted for. Typically, defects lead to local changes in the polarizability of the host, which in return modify the local field acting on the impurity. Just like local inhomogeneities (occurring over distances comparable to the lattice constant a), mesoscopic inhomogeneities ($a \ll d \ll \lambda$) affect the local field as well. A commonly used approach to interpret results in disordered heterogeneous media involves the calculation of an effective refractive index [2, 15]. As a consequence, one mesures values that are averaged over different local environments when dealing with ensemble measurements. Such average values are subsequently connected to the effective refractive index of the matrix, but this procedure may become invalid when dealing with single impurities or individual nanoparticles. For a single particle close to a mesoscopically heterogeneous entity, a full calculation of the scattered field is usually needed to account for local-field corrections, which also includes retardation effects. In general, environmental fluctuations always occur due to the mobility of species. Information at the local level (spatially and temporally) is accessible for measurement times smaller than typical diffusion times. In solids, this can happen when dealing with mesoscale entities at room temperature, or at molecular scales at ultra-low temperature [7, 25, 37–39]. In liquids or gases (with much smaller viscosities), diffusion is much faster and complicates direct local measurements, such that either ensemble or time averaging procedures are often unavoidable.

In practice, the distance of influence of the medium on guest molecules is not infinite. Toptygin [1] defines a typical cut-off distance from a probe dipole over which the influence of the environment can be neglected, which is crucial for the use of luminescent particles as nanoprobes of refractive index [6, 7, 9]. Such considerations have therefore led to new efforts for extending the definition of a local effective refractive index to complex soft-matter systems, in which the exact guest-host geometry is usually not known [5, 9, 39] and can furthermore change over time.

For absorbing media, corrections to both models of empty-cavity and Lorentz cavity are needed and the radius of the cavity no longer cancels out in the local-field correction factor, as derived by Scheel et al. [40, 41].

3.8 Experimental investigations of local-field effects

We will now review illustrative experiments for the influence of local-field effects on the spectroscopic properties of different types of host-guest systems and discuss their interpretation in the spirit of the Onsager–Böttcher model.

3.8.1 Rare earth ions in bulk systems

Rare earth (RE) ions embedded in different hosts have been widely studied, notably due to their rich electronic structure, which is well understood for the isolated ions. However, the interpretation of spectroscopic properties of RE ions in solids has sometimes remained controversial because the influence of the host matrix tends to affect the optical transitions of the ions considerably. Experiments were therefore performed in glassy structures [42–44], where the refractive index can be changed by simply varying the volume fractions of the glass constituents. Rare-earth ions are known to possess a relatively low polarizability in general [42, 45]. Therefore, the empty-cavity model has been found to mostly apply. In Ref. [44] it was determined that the Dy ion replaces a host atom and creates a tiny, but actual void in the matrix (substitutional site) of covalently bound chalcogenide glass, in agreement with the empty-cavity picture. The same behavior was encountered for Eu^{3+} ions in a PbO-B_2O_3 glass system [42,43]. In this case, the low-polarizability RE ion substitutes a Pb site with high polarizability, and therefore distorts the matrix. One interesting idea in Ref. [42] is the use of the polarizability as an adjustable parameter in the model given by (8), where a very low value was found for χ, further confirming the applicability of the EC model.

A reinterpretation of experimental results in the framework developed by Lagendijk and coworkers was carried out notably by Duan et al., [45], including the cases of a Eu^{3+}-hfa-topo complex [46,47], Ce^{3+} in different hosts [48], Eu^{3+} in glass systems [42], and yttrium oxide Y_2O_3 nanoparticles [37]. It was found that, contrary to the systems discussed in the beginning of this section, the virtual-cavity model can be applied to Ce^{3+} ions dispersed in different hosts. The proposed explanation for this phenomenon hinges on the fact that Ce^{3+} ions replace matrix cations with low polarizability as compared to their anionic counterparts. As the local field is predominantly due to the anions, it was argued that the low-polarizability Ce^{3+} ions essentially act as interstitial impurities.

The influence of absorbing media on the local-field factor were first discussed by Scheel et al. [40,41]. In this case, corrections to both the empty-cavity and the virtual-cavity model are necessary, and the radius of the cavity no longer cancels out in the local-field correction factor. As an experimental verification, Kumar et al. [43] have studied the evolution of the luminescence of Eu^{3+} ions embedded in matrices co-doped with Nd^{3+} ions. Energy transfer occurs between the two entities, and the matrix must therefore be described using a complex refractive index. As has been mentioned above, one interesting experimental aspect is that the radius of the cavity can assume the role of a fit parameter when the absorption of the matrix is varied. A cavity radius of about 1 nm was thus found, in very good agreement with the characteristic distance of absorption for rare earth ions [43].

A further illustration of the importance of cavity shape and microscopic host-guest interactions is provided by investigations of the local-field effects on

the lifetime of an $Eu(fod)_3$ complex [49], which show strong deviations from the predictions of a model with a fixed cavity shape. As pointed out in Ref. [1], this behavior could in fact be caused by hydrogen bonding of the fluorescent species with the solvent, which breaks the spherical symmetry of the RE-containing complex.

3.8.2 Rare-earth doped nanoparticles

For dopant ions in nanoparticles (NPs), optical transitions are localized and not affected by quantum confinement – contrary to the case of semiconductor quantum dots discussed later. In most cases, experimental results are in good agreement with the empty-cavity model [45–47, 50–52]. This concordance often arises from an actual cavity being created in the host matrix (substitutional case) by the impurity, which has a low polarizability compared to the host constituents. The first observations of lifetime modification of RE ions dispersed in nanostructures were in fact interpreted in terms of a change in the local effective refractive index, taking the volume fraction of the different dielectric constituents as adjustable parameters [37, 45].

More recently, Senden and coworkers performed experiments on the luminescence lifetime of $LaPO_4$ NCs doped with Ce^{3+} and Tb^{3+} ions [4]. They adapted the EC model to a more complex cavity model, where the inner refractive index is included to account for the variation of lifetime, see Eq. (13), and showed that this electrostatic model remains valid with less than 5% error for nanocrystal sizes up to 40 nm.

It has furthermore been reported that, once the NP size drops below a certain threshold, the lifetime of embedded RE ions starts to depend on the size of the nanocrystal [25, 52]. This observation raises an important point: Although the cavity model does not contain any dependence on the absolute NP size, the local field factor should be influenced by the ratio of the radii of the NP and the Onsager cavity in which the emitter is situated. To describe the actual modification of the dopant radiative rate, and to eventually compare it for different kinds of NPs, one should generalize the derivation of Eq. (13) to a core-shell system of a nanoparticle containing the Onsager cavity [28, 29]. An increasing nanoparticle size thus changes the local-field factor, even though the host material remains unchanged. Note that this consideration becomes irrelevant when the impurity has the same polarizability as the NP constituents (Lorentz local field). The case of NPs thus raises new challenges for the comprehension of local field effects, where new variables such as the NP material or its size must be considered.

3.8.3 Single organic chromophores

Similar results as for the case of RE-doped NCs had previously been observed for fluorescent molecules dissolved in water droplets (size ≈ 2 nm). Using a core-shell model comprising the surfactant layer, the authors of Refs. [53] and [54] showed that the empty-cavity model is suitable for describing the evolution of the local field experienced by Sulforhodamine B and Sulforhodamine 101. This result is in agreement with the very low increase in the polarizability density inside the droplet due to the molecules, which typically possess a polarizability of around 60 $Å^3$, small compared to the volume of the droplets.

Later, Vallée et al. [24] developed an approach based on the Onsager–Böttcher model to study the lifetime dynamics of DiD molecules in polymers. The molecule in this case is surrounded by a fluctuating environment of monomers, as it is immersed in a polymeric matrix. It was shown that the local field is strongly affected by the local dielectric fluctuations around the emitter. The subsequent calculation of the reaction field due to the molecule in different matrix configurations provides access to the total modification to the dipole moment of the molecule and explains the observed variations of lifetime. Vallée et al. furthermore found that continuum behavior is reached only after considering a few solvation shells, stressing the importance of near-field dipole interactions. Note that, as mentioned in Section 3.7.3, the distinction between the models in this situation is irrelevant, since the surrounding medium is inhomogeneous. Nevertheless, the empty-cavity factor could be applied considering the fluctuations as variations of an effective refractive index experienced by the chromophore [38].

The local-field factor can furthermore be probed by analyzing the zero-phonon line (ZPL) of single molecules. At low temperature the width of the transition is solely limited by the natural lifetime. In Ref. [7], optical spectroscopy of single terrylene molecule dispersed in various polymeric matrices was studied. The authors concluded that the variations of the ZPL width can be explained by both the EC and VC models, so that further experiments may be needed to discriminate between these two models.

Finally, Rebane and coworkers [8] used a combination of one- and two-photon absorption measurements to determine the polarizability and dipole moment of the Prodan and C153 chromophores. A significant red-shift of the absorption with increasing dielectric constant of the medium was observed. Based on the previously described Onsager–Böttcher model, the authors were able to determine the dipole moments of the excited and ground states, the polarizabilities, the radius of the cavity, as well as the strength of the reaction field, found to be of the order $0 - 10^7 \mathrm{V\ cm^{-1}}$. This analysis illustrates the power of the Onsager–Böttcher picture for extracting important electronic properties of molecules.

3.8.4 Semiconductor quantum dots

Quantum-confined structures are increasingly popular, owing to the tunability of optical properties by changing size, geometry, and structure. In such nanostructures, the optical properties are a result of the quantum confinement effect experienced by the optically generated exciton (electron-hole pair). Quantum Dots (QDs) are characterized by 3D confinement of the exciton, as compared to quantum wires (2D) or quantum wells (1D). The situation is thus different from the case of RE ions doped nanoparticles, since in QDs the crystal structure itself is an integral part of the emission process, with the exciton delocalized in the core of the nanocrystal. Only few experiments have investigated the influence of local field effects in homogeneous, dense dielectric media on quantum confined structures [9, 55, 56], and no definitive conclusion has been reached so far.

Recently, Hens et al. [57] have shown that light absorption above the band gap is well described by standard local-field models, but the quantum confinement effects render difficult the extension to near-bandgap transitions. For emission, a real-cavity model considering the inner refractive index of the QD has been proposed [58]. However, this treatment still poses the fundamental

problem of predicting a non-zero transition probability when the inner refractive index is zero, which has no physical meaning in case of the QDs: Such an emitter should be considered as a whole, and no separation between the exciton and the structure "hosting" it can be justified.

First experiments on lifetime variations of CdSe and CdTe QDs were performed by Wuister and coworkers [56]. They found the Crenshaw–Bowden model [32] to be most suitable for interpreting their experimental data, although this model has remained controversial [33], as discussed above. Moreover, the small overall variation of lifetime within the range of different refractive indices that could be studied, combined with the unknown exact quantum yield, made an unambiguous rejection of the empty-cavity model difficult [45].

More recently, Aubret et al. [9] have investigated the local-field effects on CdSe/ZnS core-shell QDs. Here, the quantum yield in vacuum was used as the crucial parameter for discriminating between the models. Unambiguously, the VC model was found to be more adequate than the empty-cavity model, in disagreement with the above-mentioned experiments.

Finally, while QDs dots are often considered as polar due to the presence of a strong permanent excitonic dipole moment alone, it has been demonstrated that they possess a very high excited-state polarizability, typically comparable to their volume [59–62], such that $\chi/(\epsilon_0 V_\mathrm{I}) \approx 1$. These two factors combined imply that the reaction field cannot be neglected, as is the case in the empty-cavity model.

4 Conclusion

We have presented an illustrative treatment of local field effects as they apply in optical spectroscopy of chromophores in dielectric media. A simplified electrostatic model based on Onsager–Böttcher theory served as a unifying framework to elucidate the fundamental link between the different local-field correction factors used in the literature. We thus saw that tuning the polarizability difference $\delta = \chi - \alpha$ between guest emitters (χ) and the atoms or molecules of the host matrix (α) mediates a gradual transition from the empty-cavity local field factor ($\chi = 0$, meaning $\delta = -\alpha$) to the Lorentz cavity (virtual cavity model), which is applicable when the guest has exactly the same polarizability as the solvent ($\delta = 0$). Further extrapolating of this trend leads to scenarios in which the guest molecule has a higher polarizability than the solvent for comparable van der Waals radii; this situation is the one most commonly encountered in single-molecule spectroscopy, given that dyes and other optically active molecules are usually placed in solutions or matrices that interact weakly with visible light and are therefore as a rule less polarizable than the solute. As the molecular polarizability χ is in general unknown, it may serve as a parameter to adjust the measurements of the same solute molecule in a variety of solvents or matrices with different dielectric permittivities ϵ, provided that the volume occupied by the molecule is known a priory or can be estimated with sufficient accuracy.

We have furthermore discussed extensions of the simple model applying to special cases such as non-spherical molecules and inhomogeneous or absorbing media, as well as complementary approaches based on microscopic models and quantum-mechanical treatments. We saw that the latter approaches offer a description at a more fundamental level, but at the cost of being restricted to

simpler systems such as highly dilute gases. Hybrid models mixing continuous-media properties like the dielectric constant of the host with microscopic properties of the guest insertion site may be useful to rationalize a given choice of model (empty cavity versus virtual cavity) in a number of systems, although it may be difficult to justify exactly where the boundary between thinking of individual atoms/molecules and treating the host as a continuous medium should be established. Finally, we have given an overview of recent experiments whose interpretation requires dealing with local field corrections, both to illustrate the models that we discussed as well as to showcase the potential of single-emitter spectroscopy in dielectric media.

5 Keywords

nano-probes, local-field correction, empty/virtual cavity model, fluorescence lifetimes in dielectrics

6 TOC

Single molecules and other nano-particles can serve as sensitive probes for condensed matter. A potential complication in the interpretation of such experiments is the field-correction factor needed to relate the local field (experienced by the probe) to its macroscopic counterpart. We review a simple conceptual framework encompassing all commonly used models for obtaining local-field factors, and we discuss experimental research that illustrates the potential of the measurement of local electric fields in dense dielectric media.

References

[1] D. Toptygin, *J. Fluoresc.* **2003**, *13*, 201–219.

[2] K. Dolgaleva, R. W. Boyd, *Adv. Opt. Photonics* **2012**, *4*, 1–77.

[3] F. T. Rabouw, S. A. den Hartog, T. Senden, A. Meijerink, *Nat. Commun.* **2014**, *5*, 3610.

[4] T. Senden, F. T. Rabouw, A. Meijerink, *ACS Nano* **2015**, *9*, 1801–1808.

[5] K. Suhling, J. Siegel, D. Phillips, P. M. W. French, S. Lévêque-Fort, S. E. D. Webb, D. M. Davis, *Biophys. J.* **2002**, *83*, 3589–3595.

[6] H. J. van Manen, P. Verkuijlen, P. Wittendorp, V. Subramaniam, T. K. van den Berg, D. Roos, C. Otto, *Biophys. J.* **2008**, *94*, L67–69.

[7] T. A. Anikushina, M. G. Gladush, A. A. Gorshelev, A. V. Naumov, *Faraday Discuss.* **2015**, *184*, 263–274.

[8] A. Rebane, G. Wicks, M. Drobizhev, T. Cooper, A. Trummal, M. Uudsemaa, *Angew. Chem.-Int. Edit.* **2015**, *54*, 7582–7586.

[9] A. Aubret, A. Pillonnet, J. Houel, C. Dujardin, F. Kulzer, *Nanoscale* **2016**, *8*, 2317–2325.

[10] R. W. Munn, *J. Chem. Phys.* **2001**, *114*, 5404–5414.

[11] R. P. Bell, *Trans. Faraday Soc.* **1931**, *27*, 797–802.

[12] D. J. Griffiths, *Introduction to Electrodynamics*, 4th ed., Pearson Education, New York, **2013**.

[13] R. J. Glauber, M. Lewenstein, *Phys. Rev. A* **1991**, *43*, 467–491.

[14] G. Mie, *Ann. Phys.-Berlin* **1908**, *330*, 377–445.

[15] D. E. Aspnes, *Am. J. Phys.* **1982**, *50*, 704–709.

[16] H. A. Lorentz, *The Theory of Electrons*, Dover Publications, New York, **1952**.

[17] C. J. F. Böttcher, *Theory of Electric Polarization*, vol. 1, 2nd ed., Elsevier, Amsterdam, **1973**.

[18] L. Onsager, *J. Am. Chem. Soc.* **1936**, *58*, 1486–1493.

[19] M. Dinpajooh, D. V. Matyushov, *Phys. Rev. Lett.* **2015**, *114*, 207 801.

[20] G. Nienhuis, C. T. J. Alkemade, *Physica C* **1976**, *81*, 181–188.

[21] R. Wortmann, D. M. Bishop, *J. Chem. Phys.* **1998**, *108*, 1001–1007.

[22] P. Macák, P. Norman, Y. Luo, H. Ågren, *J. Chem. Phys.* **2000**, *112*, 1868–1875.

[23] R. W. Munn, Y. Luo, P. Macák, H. Ågren, *J. Chem. Phys.* **2001**, *114*, 3105–3108.

[24] R. A. L. Vallée, M. Van Der Auweraer, F. C. De Schryver, D. Beljonne, M. Orrit, *ChemPhysChem* **2005**, *6*, 81–91.

[25] R. S. Meltzer, W. M. Yen, H. R. Zheng, S. P. Feofilov, M. J. Dejneka, B. Tissue, H. B. Yuan, *J. Lumines.* **2001**, *94*, 217–220.

[26] M. Y. Balakina, *ChemPhysChem* **2006**, *7*, 2115–2125.

[27] L. Novotny, B. Hecht, *Principles of Nano-Optics*, 2nd ed., Cambridge University Press, Cambridge, **2012**.

[28] C. Q. Cao, W. Long, H. Cao, *Phys. Lett. A* **1997**, *232*, 15–24.

[29] M. S. Tomaš, *Phys. Rev. A* **2001**, *63*, 053 811.

[30] P. de Vries, A. Lagendijk, *Phys. Rev. Lett.* **1998**, *81*, 1381–1384.

[31] F. J. P. Schuurmans, P. de Vries, A. Lagendijk, *Phys. Lett. A* **2000**, *264*, 472–477.

[32] M. E. Crenshaw, C. M. Bowden, *Phys. Rev. Lett.* **2000**, *85*, 1851–1854.

[33] P. R. Berman, P. W. Milonni, *Phys. Rev. Lett.* **2004**, *92*, 053 601.

[34] H. Fu, P. R. Berman, *Phys. Rev. A* **2005**, *72*, 022 104.

[35] M. E. Crenshaw, *Phys. Rev. A* **2008**, *78*, 053 827.

[36] J. Tomasi, B. Mennucci, R. Cammi, *Chem. Rev.* **2005**, *105*, 2999–3093.

[37] R. S. Meltzer, S. P. Feofilov, B. Tissue, H. B. Yuan, *Phys. Rev. B* **1999**, *60*, 14 012–14 015.

[38] R. A. L. Vallée, N. Tomczak, G. J. Vancso, L. Kuipers, N. F. van Hulst, *J. Chem. Phys.* **2005**, *122*, 114 704.

[39] V. LeBihan, A. Pillonnet, D. Amans, G. Ledoux, O. Marty, C. Dujardin, *Phys. Rev. B* **2008**, *78*, 113 405.

[40] S. Scheel, L. Knöll, D. G. Welsch, *Phys. Rev. A* **1999**, *60*, 4094–4104.

[41] S. Scheel, L. Knöll, D. G. Welsch, S. M. Barnett, *Phys. Rev. A* **1999**, *60*, 1590–1597.

[42] G. M. Kumar, D. N. Rao, G. S. Agarwal, *Phys. Rev. Lett.* **2003**, *91*, 203 903.

[43] G. M. Kumar, D. N. Rao, G. S. Agarwal, *Opt. Lett.* **2005**, *30*, 732–734.

[44] Y. G. Choi, J. H. Song, *Chem. Phys. Lett.* **2009**, *467*, 323–326.

[45] C. K. Duan, M. F. Reid, Z. Q. Wang, *Phys. Lett. A* **2005**, *343*, 474–480.

[46] G. L. J. A. Rikken, Y. A. R. R. Kessener, *Phys. Rev. Lett.* **1995**, *74*, 880–883.

[47] F. J. P. Schuurmans, D. T. N. de Lang, G. H. Wegdam, R. Sprik, A. Lagendijk, *Phys. Rev. Lett.* **1998**, *80*, 5077–5080.

[48] C. K. Duan, M. F. Reid, *Curr. Appl. Phys.* **2006**, *6*, 348–350.

[49] F. J. P. Schuurmans, A. Lagendijk, *J. Chem. Phys.* **2000**, *113*, 3310–3314.

[50] K. Dolgaleva, R. W. Boyd, P. W. Milonni, *J. Opt. Soc. Am. B-Opt. Phys.* **2007**, *24*, 516–521.

[51] E. J. He, H. R. Zheng, X. S. Zhang, S. X. Qu, *Luminescence* **2010**, *25*, 66–70.

[52] X. J. Xue, Z. C. Duan, T. Suzuki, R. N. Tiwari, M. Yoshimura, Y. Ohishi, *J. Phys. Chem. C* **2012**, *116*, 22 545–22 551.

[53] P. Lavallard, M. Rosenbauer, T. Gacoin, *Phys. Rev. A* **1996**, *54*, 5450–5453.

[54] G. Lamouche, P. Lavallard, T. Gacoin, *Phys. Rev. A* **1999**, *59*, 4668–4674.

[55] E. Yablonovitch, T. J. Gmitter, R. Bhat, *Phys. Rev. Lett.* **1988**, *61*, 2546–2549.

[56] S. F. Wuister, C. D. Donegá, A. Meijerink, *J. Chem. Phys.* **2004**, *121*, 4310–4315.

[57] Z. Hens, I. Moreels, *J. Mater. Chem.* **2012**, *22*, 10 406–10 415.

[58] A. Thränhardt, C. Ell, G. Khitrova, H. M. Gibbs, *Phys. Rev. B* **2002**, *65*, 035 327.

[59] S. A. Empedocles, M. G. Bawendi, *Science* **1997**, *278*, 2114–2117.

[60] F. Wang, J. Shan, M. A. Islam, I. P. Herman, M. Bonn, T. F. Heinz, *Nat. Mater.* **2006**, *5*, 861–864.

[61] K. Park, Z. Deutsch, J. J. Li, D. Oron, S. Weiss, *ACS Nano* **2012**, *6*, 10 013–10 023.

[62] J. D. Mar, J. J. Baumberg, X. L. Xu, A. C. Irvine, D. A. Williams, *Phys. Rev. B* **2017**, *95*, 201 304.

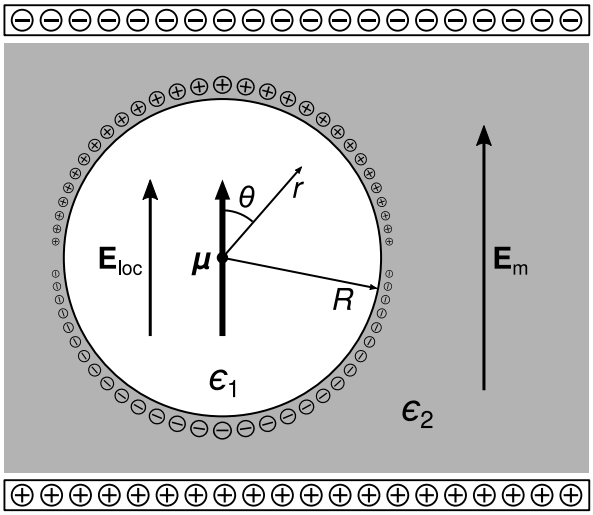

Figure 1: Schematic representation of a dielectric material under the influence of a macroscopic field $\mathbf{E}_{\rm m}$ (drawing not to scale). Individual atoms or molecules in the medium are modeled as a spherical cavity of radius R containing a single point dipole μ at its center, induced by the local field $\mathbf{E}_{\rm loc}$. Fields and potentials are expressed in polar coordinates centered on the point dipole as indicated, namely the distance r and the polar angle θ. (The system is invariant with respect to the azimuthal angle ϕ.)

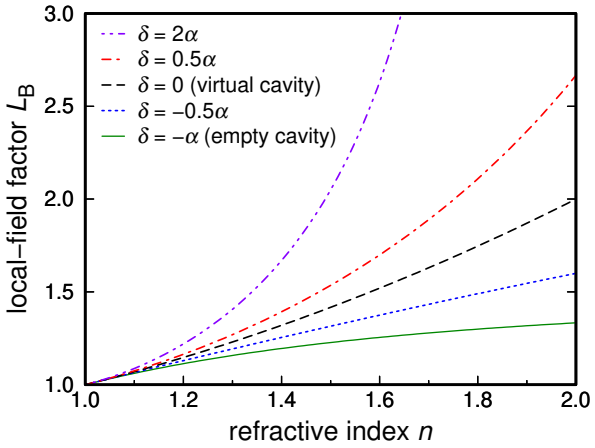

Figure 2: The local-field factor $L_{\rm B}$ as given in Eq. (13) for different values of the polarizability difference $\delta = \chi - \alpha$. For $\delta = -\alpha$, one finds the empty cavity factor, while for $\delta = 0$, the Lorentz factor is recovered. The factor $L_{\rm B}$ is plotted as a function of the refractive index of the solvent in the optical region, $n = \sqrt{\epsilon_2}$.

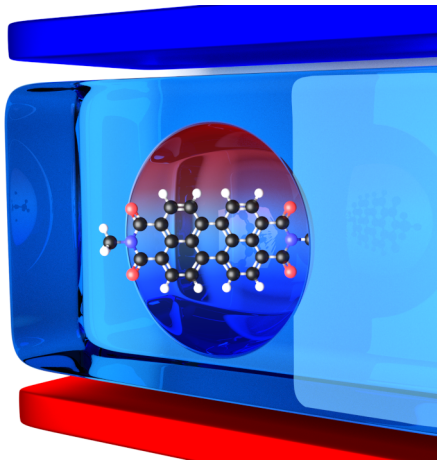

Figure 3: TOC figure.